Contrib Mineral Petrol (1982) 81:219–229

Contributions to Mineralogy and Petrology

Numerical Simulations of Crystallization Processes of Plagioclase in Complex Melts: the Origin of Major and Oscillatory Zoning in Plagioclase

Timothy P. Loomis
Department of Geosciences, University of Arizona, Tucson, Arizona 87521, USA

Abstract. Numerical simulations of the growth of a large crystal face of plagioclase in response to an instantaneous undercooling below the equilibrium temperature are presented for model granodiorite and basalt melts with varying water contents. The simulations suggest that the anorthite content of plagioclase decreases uniformly from the composition in equilibrium with the bulk melt as undercooling is increased, and that the water content in the melt has little influence on this result. Comparison of the simulations with sharp compositional changes in natural profiles suggests that undercoolings of tens of degrees C can be rapidly imposed on plutonic phenocrysts. Large changes of undercooling most likely result from chilling of the magma and local convection around growing crystals. The observation in experiments that growth rate does not increase rapidly with increasing water content in the starting melting composition can be attributed to the concentration of water at the crystal face during growth; the action of water to reduce liquidus temperature and undercooling has a greater effect on growth rate than its action to increase transport rates. Even at large undercooling, there is no significant increase in temperature at the interface caused by the release of heat of crystallization.

Simulations are presented to illustrate how disequilibrium growth processes due to undercooling can modify the normal zoning profiles expected from fractionation. Assuming that an undercooling is necessary to cause nucleation, normal zoning can result if crystal growth takes place at constant or increasing undercooling, but reverse zoning can occur at decreasing undercooling. Undercooling during growth is controlled by the relative rate of cooling and the rate at which the liquidus temperature is decreased by the accumulation of residual components and volatiles in the melt. Consequently, normal zoning should be promoted by rapid cooling, contemporaneous crystallization of other phases, and absence of volatiles, while reverse zoning should be expected in phenocrysts grown in slowly-cooled melts or in melts where volatiles are concentrated. The zoning patterns found in many plutonic plagioclase crystals suggest that their compositions are in significant disequilibrium with the melt; consequently, they are unsuitable for use in geothermometers.

Approximate calculations suggest that the amount of water concentrated at the surface of growing phenocrysts in plutons can promote local convection. Comparison of simulated and observed oscillatory zoning profiles suggests that oscillatory zoning is not explained by a re-nucleation-diffusion model (Harloff 1927), but is readily explained by periodic local convection.

Introduction

Compositional zoning of plagioclase in igneous rocks is potentially a valuable tool for understanding the changing chemical and physical conditions prevailing during solidification of magmas and the consequent release of volatiles. The usefulness of plagioclase zoning in recording igneous history derives from the wide compositional variation possible and the sensitivity of composition to chemical and physical conditions. Plagioclase is a stable phase in many natural magmas throughout crystallization.

Compositional zoning can be explained in terms of two end-member processes. Regular, normal zoning can be created by equilibrium fractionation ("Rayleigh fractionation") if diffusion within the crystal is negligible and if components are unequally distributed at equilibrium between melt and crystal. Equilibrium fractionation, as used here, is considered to be an "equilibrium" process because the surface of a growing crystal remains in equilibrium with the bulk melt composition. A second class of processes is termed "disequilibrium" because the surface of the crystal is not in equilibrium with the bulk melt, although local equilibrium at the crystal-melt interface may or may not prevail. Disequilibrium processes are known to occur in many experimental systems and may explain irregular zoning commonly found in plagioclase.

The first part of this paper presents a detailed examination of disequilibrium growth processes at the plagioclase crystal surface. The complexity of the simulation procedure necessitates neglecting fractionation of the bulk melt. The second part presents simulations of the equilibrium fractionation process and simulations that demonstrate how a combination of both fractionation and disequilibrium processes can produce the irregular and reverse zoning commonly observed in plagioclase. The third part considers geological applications of these models.

Disequilibrium growth of a solid solution crystal from a natural melt involves the interaction of several equilibrium and kinetic processes. The complexity of interaction of these processes makes it difficult to assess qualitatively the effect of geological variables, such as melt composition and temperature, on crystal composition. Moreover, the

0010-7999/82/0081/0219/$02.20

difficulty of conducting successful kinetic experiments at low undercooling and without fractionation of the charge indicates that experimental data on disequilibrium processes will be slow in coming. Consequently, I have pursued numerical similations of disequilibrium crystallization as a means of identifying the probable influence of geological variables on plagioclase composition. The present paucity of kinetic data and the modeling assumptions made for tractability purposes limit the accuracy of the simulations, but I believe that the results are useful for interpreting plagioclase zoning in terms of magmatic processes. The work reported here is an extension of modeling conducted for the plagioclase-water system (Loomis 1981) to complex natural compositions. The modeling methods used here are discussed in detail in the previous paper and are summarized here. In particular, I will emphasize differences from earlier models that result from changes in melt composition. The conclusions of this work are applied to a natural example of plagioclase zoning in a granodiorite pluton in another paper (Loomis and Welber 1983).

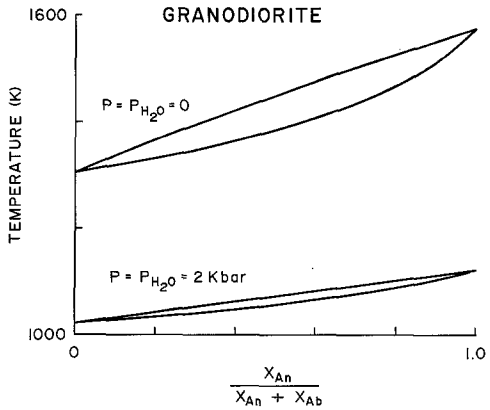

Fig. 1. Phase diagrams for plagioclase in a melt of variable An/Ab ratio but with total An+Ab content equal to that in composition G, computed using an empirical model (Loomis 1979). *Top:* dry melt at atmospheric pressure; *Bottom:* melt saturated ($X_w^m = 0.5$) at 2 Kbar pressure

Disequilibrium Growth Processes

Construction of Simulations

The numerical simulations are carried out for the growth of a flat crystal face of infinite lateral extent. This geometry is appropriate for comparison with natural phenocrysts, where compositional zoning in a direction normal to a large face is uniform across the face, and with euhedral crystals grown experimentally at small undercooling. The melt is assumed to be semi-infinite in extent. Initially, the system is at the liquidus temperature for the bulk melt composition, the melt is homogeneous, and the initial crystal interface is assumed to be of the appropriate equilibrium composition. The temperature of the entire system is instantaneously decreased by an amount corresponding to the bulk undercooling (ΔT_B) to initiate growth of the crystal face. This new temperature and the initial bulk composition of the melt are maintained at infinite distance from the crystal interface as boundary conditions on the system while growth occurs.

Two types of disequilibrium growth models were described in detail for the plagioclase-water system (Loomis 1981). In the melt-transport controlled growth model, it is assumed that the melt composition at the interface changes from the initial bulk composition to a composition corresponding to the liquidus for the actual temperature at the interface. (The interface temperature is determined by heat production at the interface, heat flow, and boundary conditions, but is very close to the temperature imposed on the system at the initiation of growth.) Local equilibrium prevails at the interface, and the composition of the crystal forming from the melt is determined by equilibrium partitioning of components. The effective undercooling *at the interface* (ΔT_I) is zero, although ΔT_B is constant. The velocity of growth in the model is governed by the rate of transport of components (and, theoretically, heat) between the interface melt and the bulk melt away from the crystal, giving rise to the name melt-transport controlled growth.

The interface-controlled growth model is similar to the first model except that the velocity of growth is limited by interface processes in addition to transport in the melt. Although more realistic than the melt-transport controlled model, the accuracy of the interface-controlled model is limited by our impoverished knowledge of (1) the relationship between velocity and the finite undercooling existing at the interface (ΔT_I), and (2) the details of non-equilibrium partitioning of components between the crystal and melt.

Both models require that the following factors and processes be represented quantitatively: plagioclase liquidus and solidus in a complex melt, equilibrium or non-equilibrium partitioning of components between melt and crystal, chemical transport in the melt, heat of crystallization, and heat flow. Diffusion within the crystal is not included because the preservation of steep compositional gradients in natural plutonic plagioclase suggests that diffusion is ineffective (see also Maaloe 1976). The methods and data used to quantify the factors and processes above, and to simulate growth according to the two growth models, are the same as described in Loomis (1981) except as discussed below.

Melt Components and Equilibrium Calculations. The composition of a complex, hydrous melt is represented in terms of the four components: An, Ab, water, and residual component. The derivation of these components from a chemical analysis is based upon the conceptual model of Burnham (1975, 1979). The residual component was normalized to 8 gram atoms of oxygen as suggested by Burnham (1975). This method of defining components was used to fit empirically equilibrium equations to experimental observations of plagioclase composition in complex melts. Thus, the definition of components and empirical equilibrium calculations are consistent with available experimental data (Loomis 1979). This equilibrium model is used in the simulations to calculate crystal composition, liquidus temperature, and thermodynamic distribution coefficient for An and Ab as functions of melt composition.

The two salient differences between plagioclase and complex melts that affect growth simulations can be illustrated by comparing Fig. 1 with the equivalent diagram for the plagioclase-water system (for example Loomis 1979, Fig. 3). Fig. 1 shows the projection of the plagioclase liquidus and solidus from a system in which the ratio An/Ab is free to vary but in which all other components are fixed at their value in the Rocky Hill Granodiorite (Table 1). Relative to the plagioclase-water system, (1) the partition-

Table 1. Anhydrous bulk compositions (wt.%) of the Rocky Hill average granodiorite (G) and oceanic tholeiite (Bas) used in modeling. Anhydrous GFW (gm/mol) for mixtures with a mole fraction of water less than 0.5 is computed as outlined in Burnham (1979), and mole fractions of An and Ab (X_{An} and X_{Ab}) are computed as discussed in Loomis (1979)

	SiO_2	Al_2O_3	TiO_2	Fe_2O_3	FeO	MnO	MgO	CaO	Na_2O	K_2O	GFW	X_{An}	X_{Ab}
G	71.50	14.40	0.44	0.74	1.71	0.05	0.74	2.50	4.30	2.77	285	0.1126	0.3682
BAS	50.28	14.85	1.91	1.74	8.86	0	6.45	10.78	3.24	0.07	337	0.2725	0.3075

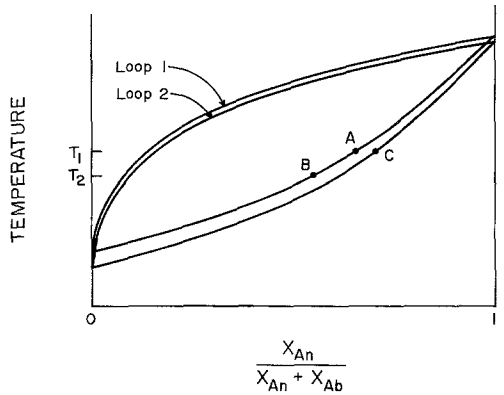

Fig. 2. Schematic plagioclase phase diagrams for complex melts showing the predictions of the non-equilibrium partitioning model. Loop 2 is a melt with greater content of the residual component or water than Loop 1

ing of An and Ab components between melt and crystal deviates less from equality, and (2) the composition of plagioclase in equilibrium with a given anhydrous melt composition does not change significantly as water is added to the system (although the equilibrium temperature changes dramatically).

Non-Equilibrium Partitioning. Interface-controlled growth involves the complication of non-equilibrium partitioning of the components An and Ab between melt and crystal. As in the preceding work, the model used predicts that the composition of crystal formed is that in equilibrium for the interface temperature regardless of the actual ratio An/Ab in the melt (Hopper and Uhlmann 1974; Loomis 1981, model 3). In a pure plagioclase melt, the equilibrium crystal composition is uniquely defined by temperature alone. However, in a complex melt, the equilibrium composition depends on the composition of the melt. For example, Fig. 1 shows that the equilibrium composition of plagioclase at a *given temperature* is very dependent on the water content of the melt. For the complex melts considered here, the equilibrium plagioclase composition at the interface temperature is calculated for a melt with the contents of water and residual component predicted to be present at the interface. Clearly other non-equilibrium partitioning models will predict different crystal compositions for a given interface temperature and melt composition, but all those investigated previously (Loomis 1981) agree in the prediction that the crystal will be more sodic than that in equilibrium with the bulk melt in these simulations.

The effects of changing temperature and melt composition on crystal composition according to the predictions of the non-equilibrium partitioning model are illustrated schematically in Fig. 2. Loop 1 shows the equilibrium plagioclase phase diagram for a complex melt with a certain content of residual component and water. Loop 2 shows the phase diagram for a melt with slightly greater content of residual component or water. According to the non-equilibrium partitioning model, a melt with the content of residual component and water of Loop 1 at temperature T_1 will crystallize plagioclase of composition A, regardless of the ratio An/Ab in the melt. If the temperature is lowered to T_2, this same melt will crystallize the more sodic plagioclase composition B. Alternatively, if the temperature remains constant at T_1 but the amount of residual component or water increases to that of Loop 2 (or equivalently, plagioclase is removed), the melt crystallizes the more calcic composition C. These pedictions are referred to in following sections of this paper to explain reverse and oscillatory zoning.

Chemical Transport. All transport in the melt is represented by the diffusion equation in these simulations. The thermodynamic components defined by the equilibrium model (An, Ab, water, and residual) are used to describe the diffusion process. This choice of components is advantageous for two reasons. First, the stoichiometric composition of plagioclase imposes a boundary condition on diffusion in the melt such that a diffusion model must ultimately describe the flux of An and Ab components. Second, the general polymerized nature of feldspar-rich melts (Flood and Knapp 1968; Hess 1970; Taylor and Brown 1979), and the successful description of the thermodynamic properties of melts in terms of ideal mixing of feldspar components (Burnham 1975, 1979, and the equilibrium model used here), suggest that feldspar components can represent closer approximations to discrete structural entities in the melt than ions. Ideally, structural and thermodynamic independence of components will minimize thermodynamic and hydrodynamic cross-coupling during diffusion and simplify compositional dependence (water, unfortunately, does interact strongly with feldspar components).

In a multicomponent melt, it is necessary to describe the individual transport of each component as a function of temperature, pressure, and composition. Data do not exist to construct a transport model of this completeness for complex melts. Thus, a number of simplifications are required. First, the transport coefficients of all four components are assumed to be equal, obviating the requirement of 6 cross coefficients. Second, transport coefficients are extrapolated as a function of temperature and composition by assuming that they are proportional to temperature and inversely proportional to viscosity, as predicted by a Stokes-Einstein model (the size of a diffusing particle is not considered). Third, the effect of pressure is not known.

The Stokes-Einstein extrapolation method was used primarily for lack of a better one (data do not exist to develop even an empirical one), but it can be justified as more appropriate for these components than for many ions, for which the Stokes-Einstein equation deriving transport coefficients from ion size has been found to be grossly in error.

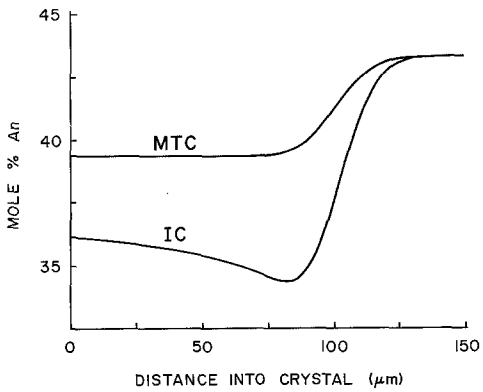

Fig. 3. Comparison of predicted crystal zoning profiles for 0.1 mm growth from composition G with 2 wt.% water, in response to an imposed ΔT_B of 25 C, according to the melt-transport controlled (MTC) and interface controlled (IC) growth models. The initial crystal composition was assumed to be in equilibrium with the bulk melt and is preserved at distances greater than 0.1 mm into the crystal

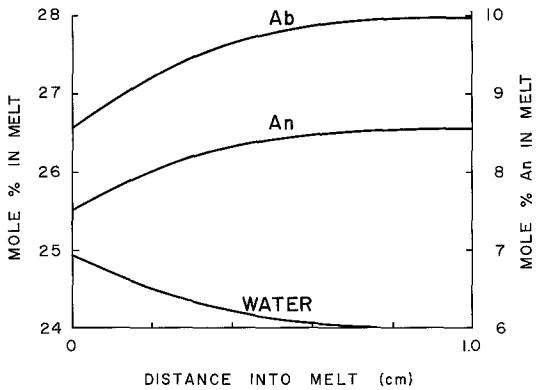

Fig. 4. Zoning profiles of components in the melt for the simulation described in Fig. 3. The null abscissa coordinate is the crystal interface. The left ordinate is the scale for Ab and water, and the right ordinate is the scale for An

The relationship between the viscosity of feldspar-rich melts and the mobility of components such as Ab and An is more obvious than between viscosity and transport of ions. The diffusivity of ions and water itself (Shaw 1974; Watson 1979) increases in response to the addition of water to the system; the simplest way to simulate this relationship is to scale the transport coefficient by viscosity.

The equation for transport of An and of Ab in dry plagioclase melts was determined previously by matching computed growth velocities of plagioclase over a range of composition and temperature to the experimental data of Kirkpatrick et al. (1979); the resulting equation was (Loomis 1981, Eq. 8):

$D = 5 \times 10^{-6}\ T/\eta$ (cm^2/s),

where viscosity (η) is in poise and T in °K. This equation is used here for the transport coefficient of all components. This equation predicts a transport coefficient for water for natural compositions that falls between the measured diffusivities by Shaw (1974) and Jambon (1979). Thus, while the transport model is of necessity a coarse approximation, it is consistent with the few available data. In view of the uncertainty in transport coefficients, they are claculated for the bulk melt composition and imposed simulation temperature and held constant everywhere throughout the simulation. The influence of possible errors in assumed transport rate on the conclusions of this paper is discussed below.

It must be emphasized that in a multicomponent diffusion system, each component can exchange with all other components. Consequently, there is no requirement that the sum An+Ab remain constant in the melt, only that the total of all components be constant.

Results and Interpretation of Disequilibrium Growth Simulations

Simulations were performed for melts for which the anhydrous compositions are given in Table 1. Composition G corresponds to the average bulk composition of the Rocky Hill Granodiorite, a pluton discussed in a subsequent paper (Loomis and Welber 1982). BAS represents an oceanic tholeiite composition. The effect of water on the crystallization process was investigated by running simulations with various amounts of water (shown as wt.%) and for saturation at 2 Kbar pressure (5.9 wt.% for composition G and 5 wt.% for composition BAS); for saturated runs, the transport coefficient of water was set to infinity to simulate vaporization of water. Another major variable of geological interest is bulk undercooling (ΔT_B). ΔT_B corresponds to the difference between the equilibrium liquidus temperature for the bulk melt composition and the actual temperature imposed on the system at the initiation of growth. All simulations were conducted until 0.1 mm of new crystal had been added. Details of the numerical simulation procedure have been presented earlier (Loomis 1981).

Growth Processes. An example of a simulation is presented in Figs. 3–5 for a hydrous granodiorite melt and a bulk undercooling of 25° C. Figure 3 shows the predicted zoning profile according to the melt-transport controlled growth model (MTC) and the interface-controlled growth model (IC) after 0.1 mm growth. As found in all simulations, the An content of the crystal drops rapidly upon initiation of growth due to the large undercooling at the crystal interface. The slow rise of An crystal composition with continued growth in the interface-controlled model is due primarily to the effect of the slowly increasing water and residual component contents at the interface on nonequilibrium partitioning, as shown in Fig. 2. The general shapes of predicted zoning profiles are similar to those simulated in the hydrous plagioclase system.

Zoning profiles of melt components are compared in Fig. 4; the residual component is the difference between unity and the sum of the three components plotted (it increases slightly toward the crystal face). The accumulation of water at the growing interface amounts to *ca.* 0.1 wt.% above the bulk composition and has important effects on growth rate, density, and viscosity. An interesting observation is that both An and Ab are depleted at the interface, whereas, in the plagioclase system, Ab is concentrated at the interface. Depletion of both components occurs in complex melts because the molar concentration of each in the melt is less than in the crystal, despite the concentration of Ab *relative* to An in the melt during growth. While the numerical prediction of depletion in this example depends on the assumption of equal molar volumes of these components in the melt and crystal, the amount of predicted deple-

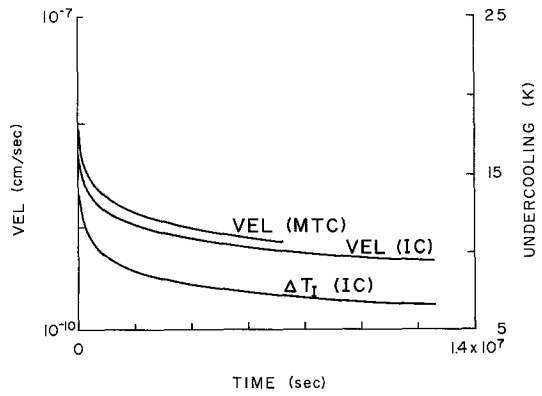

Fig. 5. Growth velocity (VEL) and effective undercooling at the interface (ΔT_I) as a function of time for the IC and MTC simulations of Fig. 3. ΔT_I for the MTC model is null

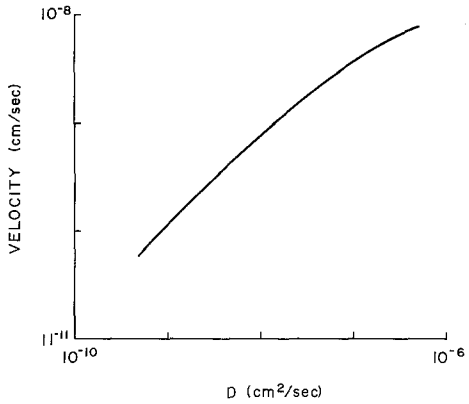

Fig. 6. The effect of varying the transport coefficient D on growth velocity after 0.1 mm growth for the IC model of Fig. 3. All other variables were held constant. The nominal value for D in the simulation of Fig. 3 was 4.7×10^{-9} cm^2/s

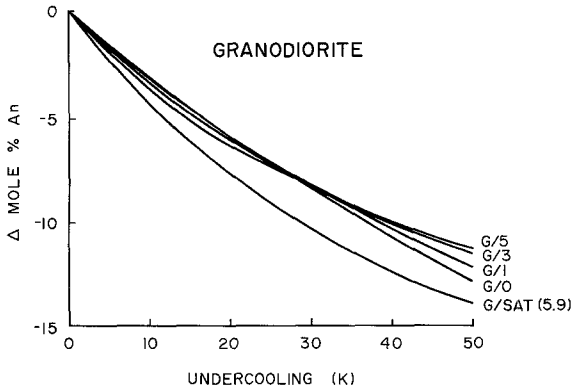

Fig. 7. Kinetic depression of An crystal composition (ΔX^x_{An}) after 0.1 mm interface-controlled growth as a function of ΔT_B and melt water content. Δ mol% An represents the interface crystal composition at the end of the simulation minus the crystal composition in equilibrium with the bulk melt composition. Granodiorite melt compositions are described by G/wt.% water or G/SAT (5.9), the latter for the saturated composition at 2 Kbar pressure with 5.9 wt.% water; the transport coefficient for water in the saturated composition was infinite

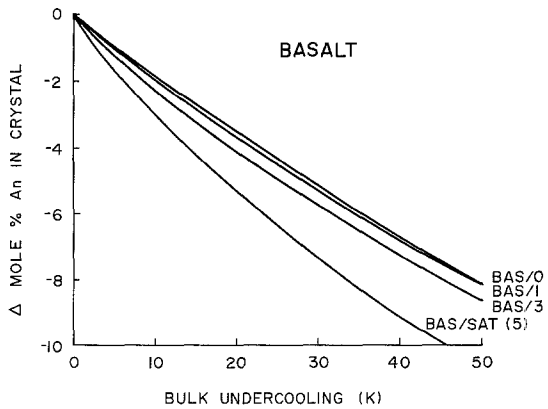

Fig. 8. Kinetic depression of An crystal composition as a function of ΔT_B and melt water content for the basalt composition (see Fig. 7 for explanation). Saturation at 2 Kbar is 5 wt.% water

tion is large enough to suggest that it should be a common result when plagioclase grows from complex melts with only a small mole fraction of An and Ab.

The heat of crystallization released during growth tends to raise the temperature at the crystal surface and reduce undercooling (ΔT_I). However, the simulation predicts that the temperature rise is less than 0.01° C, indicating that the heat of crystallization is effectively removed from the crystal interface by conduction.

The relationships among velocity, undercooling at the interface (ΔT_I), and time, shown in Fig. 5, are similar to those found for the plagioclase and plagioclase-water systems, although the absolute growth velocities in complex melts are orders of magnitude smaller. The nearly identical trends of growth velocity with time in both the MTC and IC growth models demonstrates that the most important process ultimately controlling growth velocity is transport in the melt. Figure 6 illustrates the sensitivity of predicted growth velocity to assumed diffusivity for this simulation. Clearly, our deficient knowledge of transport rates of important mineral constituents in natural melts severely limits the accuracy of simulations. On the other hand, Fig. 6 illustrates that transport rates could be derived from crystal growth experiments, although it could take almost half a year to grow 0.1 mm of crystal in this example.

Effect of Geological Variables. The effect of the major geological variables of (1) anhydrous bulk composition, (2) water content in the melt, and (3) ΔT_B, on crystal growth are reported in Figs. 7–10 and Table 2. All simulations were computed using the interface-controlled growth model, and the data reported represent conditions after 0.1 mm growth. The composition parameter reported for plagioclase is ΔX^x_{An}: the interface composition at the end of the simulation minus the composition in equilibrium with the bulk melt.

Figures 7 and 8 show that ΔT_B depresses the An-content of plagioclase a similar amount in compositions G and BAS despite the pronounced differences in growth velocity, transport coefficient, and equilibrium crystal composition. The similarity can be explained most easily by reference to the partitioning model, in which the crystal composition is determined by the interface temperature. Since the *shape* of the solidus is similar for both G and BAS compositions, decreasing the temperature an equal amount should have a similar effect on crystal composition.

The effect of ΔT_B on water accumulation at the surface

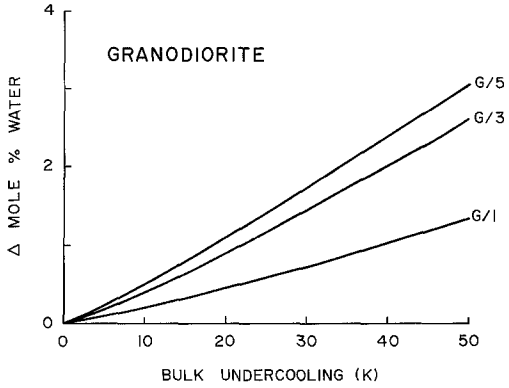

Fig. 9. Accumulation of water at the crystal interface as a function of ΔT_B and melt water content after 0.1 mm interface-controlled growth. Δ mol% water represents the interface water composition minus the bulk melt composition. The granodiorite melt composition is labeled G/wt.% water

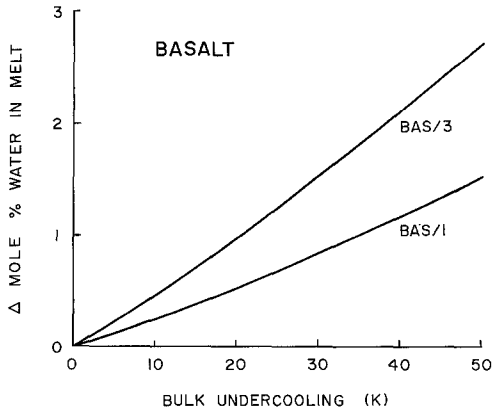

Fig. 10. Accumulation of water at the crystal interface as a function of ΔT_B and melt water content after 0.1 mm interface-controlled growth. The basaltic melt composition is given by BAS/wt.% water

Table 2. Comparison of growth models at an initial undercooling of 30° C for melt compositions (COMP) designated G (Rocky Hill Granodiorite) or BAS (olivine tholeiite)/wt.% water

COMP	FVEL (cm/s $\times 10^8$)	IVEL (cm/s $\times 10^8$)	EQUIL X^x_{An}	ΔX^x_{An}	EQUIL X^m_w	ΔX^m_w	IVISC (poise $\times 10^{-3}$)	D ($cm^2/s \times 10^7$)	T_{liq} (°K)
G/0	0.015	0.41	0.4592	−0.0844	0	0	9,930	0.0068	1,375
G/1	0.031	1.1	0.4450	−0.0831	0.14	0.0073	3,560	0.018	1,308
G/3	0.13	7.4	0.4215	−0.0824	0.33	0.0145	548	0.11	1,212
G/5	0.45	35	0.4029	−0.837	0.45	0.0173	116	0.48	1,145
G/SAT (5.9)	1.2	75	0.3943	−0.1023	0.50	0	54	1.0	1,116
BAS/0	424	9,700	0.7293	−0.0513	0	0	0.418	170	1,493
BAS/1	255	9,000	0.7151	−0.0528	0.16	0.0083	0.450	150	1,399
BAS/3	191	12,000	0.6907	−0.0575	0.37	0.0152	0.343	180	1,268
BAS/SAT (5.0)	355	20,000	0.6704	−0.0736	0.50	0	0.202	280	1,179

FVEL: velocity after 0.1 mm growth; IVEL: initial growth velocity; EQUIL X^x_{An}: mole fraction of An in plagioclase in equilibrium with the initial melt composition; ΔX^x_{An}: surface crystal composition after 0.1 mm growth minus EQUIL X^x_{An}; EQUIL X^m_w: mole fraction of water in the initial (bulk) melt; ΔX^m_w: mole fraction water in the melt at the crystal surface after 0.1 mm growth minus EQUIL X^m_w; IVISC: viscosity of melt at the crystal surface just after growth begins; D: transport coefficient of all components (except the transport coefficient of water for saturated compositions is ∞); T_{liq}: liquidus temperature for the initial melt composition

of growing crystals is also similar in G and BAS compositions (Figs. 9 and 10). The similarity can be rationalized by noting that water has a similar effect on the plagioclase liquidus temperature for both compositions. Thus, an equivalent amount of water would be expected to accumulate at the crystal interface to cancel the driving force of a given ΔT_B in the two systems. A useful corollary of this explanation is that the growth velocity of plagioclase in various melts with the same water content is approximately inversely proportional to the transport coefficient of water, as can be seen in the data of Table 2.

The foregoing observations suggest that the effects of ΔT_B on crystal composition and water accumulation at the interface can be rather simply related to the equilibrium state and partitioning laws.

The effect of water content in the bulk melt on ΔX^x_{An} is remarkably small for both compositions, except where infinite diffusivity of water for saturated compositions inhibits the accumulation of water at the crystal face (Figs. 7 and 8). This result is in contrast to that in the plagioclase-water system, where increasing water content reduced the absolute magnitude of ΔX^x_{An}. The difference between systems is not obviously explained by any simple parameter, but must be due to a combination of factors.

Figures 9 and 10 demonstrate that an increasing abundance of water in the bulk melt results in a greater accumulation of water at the crystal face for a given ΔT_B; a similar result was found for the plagioclase-water system. Increased water content in the bulk melt has two pertinent effects: it enhances the transport rate of water and it increases the amount of water that is pushed ahead of the growing crystal face. The latter effect is dominant according to the data used in these simulations.

Two predictions of the simulations can be tested by comparison with the experimental data of Swanson (1977). Swanson measured growth velocities of approximately 1×10^{-7} and 4×10^{-7} cm/s at 50 and 100 C undercooling, respectively, for plagioclase growing in a synthetic granodiorite melt with 6.5 wt% water. Interface-controlled growth simulations predict average velocities for the first 0.1 mm

water. Interface-controlled growth simulations predict average velocities for the first 0.1 mm growth of 3×10^{-8} and 2×10^{-7} cm/s at corresponding undercoolings. Swanson's data are subject to the usual experimental problems of melt fractionation, interference of crystals, and uncertainty as to the time of nucleation; moreover, the measured velocities may be greater than simulated because the experimental crystals may have assumed shapes that reduce diffusion distances. Swanson's data (Fig. 3) show a scatter of about a log unit.

In view of the experimental uncertainties, as well as the many inherent in the numerical simulations, simulations show acceptable agreement with experimental measurements. Because the simulated growth velocity is sensitive to the assumed transport coefficient, as illustrated in Fig. 6, this comparison suggests that my assumed transport rate for the synthetic melt used by Swanson cannot be many orders of magnitude in error.

Another prediction of the simulations consistent with available experimental evidence is the limited effect of water content on growth rate. Table 2 lists the growth velocity after 0.1 mm growth ("FVEL") in composition G for water contents ranging from none to *ca.* 5.9 wt.%, saturation at 2 Kbar. The bulk undercooling was 30 C in all simulations. The velocity increases only by a factor of 30 with the addition of 5 wt.% water, even though the initial velocity changes by a factor of 85 in response to changes of transport coefficient and viscosity by factors of 71 and 0.01, respectively. The limited influence of water on growth rate in the simulations is easily explained by the increased accumulation of water at the crystal face that results from increased water content of the melt, despite reduced viscosity and increased transport coefficient (Fig. 9). Water accumulation depresses the liquidus and reduces undercooling at the interface (ΔT_I), thereby reducing growth velocity according to the interface-controlled growth model.

The data of Swanson (1977) suggest that the growth rate of plagioclase at a constant undercooling decreases with increasing water content. The data of Fenn (1977) indicates that the *maximum* growth rate of alkali feldspar decreases with increasing water content, but that the growth rate at small, *constant undercooling* may stay about the same or increase slightly. Their observations suggest that the accumulation of water at a crystal face and its effects on growth processes, illustrated by the simulations, are realistic predictions. If we ignore the uncertainties inherent in the experiments and assume that the experimental observations are accurate, the simulations can be made to show an actual decrease of velocity with increased water content by decreasing diffusivity to values less than presently assumed. The interface-controlled growth equation (Loomis 1981, Eq. 1; Kirkpatrick et al. 1976) also is undoubtedly affected by water content in the melt.

It is apparent from the time scale on Fig. 5, and from the observations of Swanson (1977) and Fenn (1977), that it will be difficult to achieve the low undercoolings and long run times necessary to duplicate the crystal morphology and growth conditions in silicic natural magmas. The data of Table 2 indicate that millimeter-sized crystals probably require times on the order of a year to grow in granodiorite melts and a day in basaltic melts at bulk undercoolings of tens of degrees. Thus, simulations play an important role in extrapolating experimental results to natural conditions.

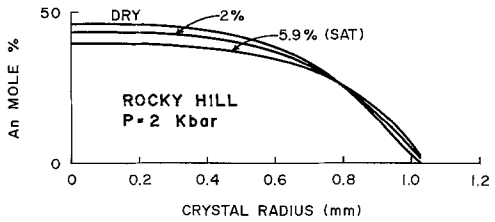

Fig. 11. Simulated equilibrium fractionation zoning profiles for plagioclase grown in the Rocky Hill granodiorite (Loomis and Welber 1982) with various water contents. The crystals are spherical and grown on 100 nuclei/cm^3 of anhydrous melt. Weight % water content of the initial melt is shown and "SAT" indicates water saturation at 2 Kbar. Water was allowed to accumulate in the residual melt until saturation was reached

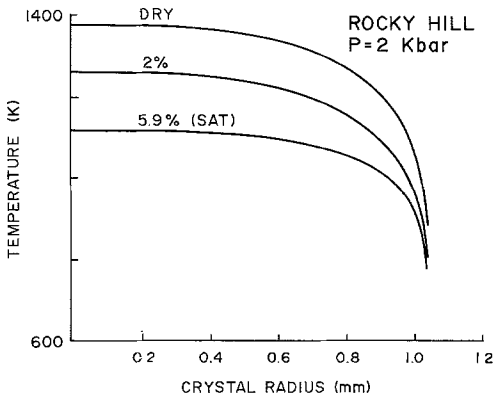

Fig. 12. Equilibrium liquidus temperature history for the simulations of Fig. 11

Fractionation Simulations

Equilibrium Fractionation

The second end-member growth process, equilibrium or Rayleigh fractionation, can be simulated as follows. Begin with one cm^3 of anhydrous melt and add enough water to produce the starting composition. Calculate the liquidus temperature of plagioclase and its composition using the empirical model of equilibrium. Assume a fixed number of nuclei of plagioclase are present and that the crystals grown are spherical. Then (1) crystallize a small amount of plagioclase onto the nuclei and calculate their radius, (2) remove the appropriate amount of An and Ab components from the melt and calculate its new composition, (3) reduce the water content of the melt, if necessary, to its saturation value, (4) recalculate the liquidus temperature and equilibrium crystal composition, and (5) repeat steps 1–4 until all An and Ab are removed from the melt. The result is an equilibrium zoning profile and a record of how the temperature varies during growth if only plagioclase crystallizes. These curves are shown in Figs. 11 and 12 for the Rocky Hill granodiorite composition (Loomis and Welber 1982) with various amounts of water.

Useful observations from these simulations are that (1) the central portion of crystals should show little zoning, (2) only continuous, normal zoning is possible by equilibrium processes, and (3) for a given cooling rate, the radial growth rate of a crystal must be much faster during early growth than later to maintain equilibrium with the melt.

Table 3. Comparison of simulated crystal compositions (Fig. 13) and experimental compositions (Lofgren 1971, Table 1, Run 68) for plagioclase grown by step cooling from a melt with 50 wt.% An and 10 wt.% water at 5 Kbar.

Interval	Temperature	Average composition		Range of composition	
	C	E	S	E	S
1	1,050	91	88	–	86–90
2	1,000	83	83	81–88	79–87
3	950	78	77	73–81	71–82
4	900	67	66	63–69	60–71
5	850	52	52	–	47–56

E: experiments; S: simulation; crystal compositions are in mol % An

These observations suggest that compositional zoning due to disequilibrium processes should be most pronounced in the inner half of the crystal radius.

Superimposed Disequilibrium

The effect of disequilibrium processes on fractionation profiles can be approximated as follows. The simultions are computed as described above except that the temperature for each growth step can be specified to be different than the equilibrium liquidus temperature. The crystal composition is then calculated using the disequilibrium partitioning model described in this paper. This procedure is a simplification of the disequilibrium growth process because transport gradients in the melt are neglected.

The superimposed fractionation and disequilibrium growth model can be tested by comparing simulations with experimentally-produced zoning profiles. Lofgren (1972) produced zoned crystals from plagioclase melts with excess water at pressures near 5 Kbar by repeatedly dropping the temperature and then holding it constant for many hours before the next temperature decrease. The crystals produced show discontinuous, reversely-zoned steps with the amount of reverse zoning increasing outward.

A simulation of his run 68 is shown in Fig. 13, and the excellent agreement with the experiments can be seen in the comparison in Table 3 (see also Fig. 2d, Lofgren 1972). The simulation was computed by dropping the temperature to the value given by Lofgren and allowing growth to continue until the liquidus temperature was equal to the actual temperature. When this equilibrium state was reached, all growth stopped until the temperature was lowered again. The simulation is based on the assumption that the water content was at saturation when growth began on each step, but that the melt adjacent to the crystal could supersaturate during growth as water was pushed ahead of the growing crystal surface. It is suggested that the long wait after growth stops at equilibrium in Lofgren's experiments provided time for water to diffuse away or to form bubbles. While Lofgren (1972, Table 1) calculated average growth rates by dividing the width of the growth steps by the time the sample was held at each temperature, the actual growth rate could have been much faster because the crystal simply stopped growing when the melt was fractionated to equilibrium. My simulations of plagioclase growth from hydrous plagioclase melts (Loomis 1981), while subject to many uncertainties, predict growth rates orders of magnitude faster than calculated by Lofgren.

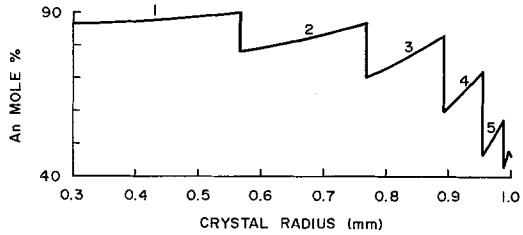

Fig. 13. Simulated plagioclase zoning for growth from a 50 wt.% An melt saturated with water at 5 Kbar pressure. Isothermal growth intervals are labeled 1–5 and compared with the experimental data in Table 3. See text for description of the simulation procedure

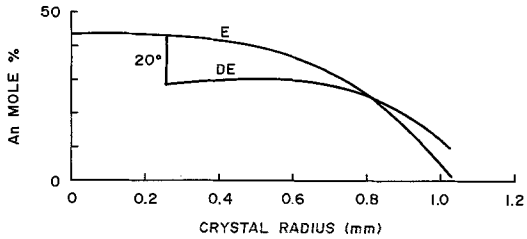

Fig. 14. Simulated plagioclase zoning for growth from the Rocky Hill granodiorite (Loomis and Welber 1982) with 2 wt.% Water. E: equilibrium fractionation identical to the 2% curve in Fig. 10; DE: disequilibrium fractionation simulation in which a 20° C undercooling was introduced at a radius of 0.25 mm and linearly decreased to zero at a radius of 1 mm

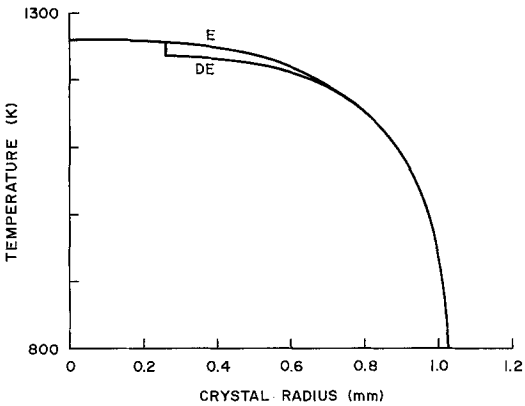

Fig. 15. Temperature history for the simulations of Fig. 14

An example of the effect of undercooling on the fractionation zoning profile of plagioclase in the Rocky Hill granodiorite is shown in Fig. 14, (profile DE), where it can be compared with the equilibrium fractionation profile (E). The temperature histories of both simulations are presented in Fig. 15. The disequilibrium profile, which looks very similar to those from plagioclase phenocrysts from the center of the pluton (Loomis and Welber 1982), was produced by allowing the crystal to grow at equilibrium until a radius of 0.25 mm was reached and then imposing an undercooling of 20° C, which was linearly decreased to zero at a radius of 1 mm. The temperature continued to decrease throughout crystallization.

The slight reverse zoning of the disequilibrium profile in Fig. 14 can be explained by reference to Fig. 2. The accumulation of the residual component and water in the melt as plagioclase is removed will tend to drive the crystallizing composition from A toward C (more calcic). At the same time, decreasing temperature will tend to drive the crystal composition toward B. In this simulation, the former effect dominates. Simulation experiments using other cooling histories indicate that (1) reversed zoning is accentuated if undercooling decreases more rapidly with growth (for example, if the temperature stays constant) and (2) normal zoning is produced if undercooling is maintained.

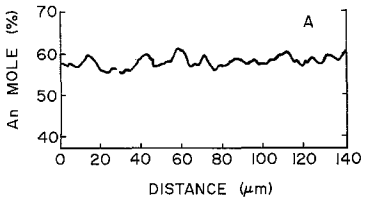

Fig. 16. Zoning profile measured from the center outward of a plagioclase crystal from a quartz diorite pluton. The microprobe step interval was 1 μm, and the profile was smoothed using a first order, three point algorithm to remove high-frequency, statistical noise

Geological Applications

Considering the assumptions necessary to simulate crystal growth in complex geological materials and the paucity of reliable experimental data, the predictions of the simulations can be considered to be only semiquantitative in significance. However, the results of simulations do have useful implications for the analysis of plagioclase growth under natural conditions.

Undercooling

The geometric boundary conditions and initial conditions of the disequilibrium growth simulations presented in the first part of this paper are directly appropriate for three gologic situations. In the first case, a crystal could be in equilibrium with a melt in a chamber at depth. Rapid cooling of the melt upon intrusion could be caused by convection and by the rapidity of heat conduction with respect to the rates of crystal growth and diffusion. The decreased temperature could impose a bulk undercooling on preexisting, large crystals. The second appropriate situation could occur if the growth of a crystal is controlled by a surface re-nucleation mechanism and requires a finite undercooling to begin, as suggested by the interpretation of oscillatory zoning put forth by Harloff (1927) and Vance (1962). If a crystal stops growing, the boundary layer in the adjacent melt would be changed to the bulk melt composition by diffusion. When re-nucleation of growth on the existing crystal face occurs, the initial conditions correspond to those of the models. The third process, that could also be responsible for oscillatory zoning, is the periodic, convective overturn of the boundary layer melt next to a growing crystal face. This process can impose a large ΔT_B by rapidly changing the melt composition.

Under the preceding circumstances, the amount of An drop at the boundaries of resorbed plagioclase cores, and the magnitude of compositional oscillations in oscillatory zoning, would be measures of the deviation of crystal composition from equilibrium. The magnitude of these variations is observed to be a few to about ten mol% An (Vance 1962; Wiebe 1968; Sibley et all 1976; Loomis and Welber 1982). The simulations presented here (Figs. 7–8) suggest that corresponding values of ΔT_B for phenocryst growth up to several tens of degrees C are possible. A corroborating estimate of undercooling is based on the nucleation data of Swanson (1977). Reasonable nucleation densities (10–100 nuclei/cm^3) for plagioclase are expected in granitic and granodiorite compositions with moderate water contents at undercoolings of this magnitude.

Oscillatory Zoning and the Instability of the Interface Melt

Oscillatory zoning is a common attribute of plagioclase phenocrysts that has recieved considerable attention (Bottinga et al. 1966; Greenwood and McTaggart 1957; Vance 1962; Wiebe 1968; Sibley et al. 1976). Harloff (1927) and Hills (1936) were two early workers who suggested that diffusion in the melt and surface nucleation growth of crystals were responsible for oscillatory zoning. Vance (1962) elaborated on the theory and suggested that oscillatory zoning could only occur in water undersaturated systems where creation of bubbles would not destory compositional gradients. Bottinga et al. (1966) show a schematic model of zoning and interpret sharp compositional variations as periods of no growth. Sibley et al. (1976) reiterate the model, referring to the boundary layer diffusion phenomenon as constitutional supercooling, after Rutter and Chalmers (1953); these later models are essentially equivalent to that proposed by Harloff (1927).

The periodic growth model of plagioclase oscillatory zoning can be evaluated by the simulations developed here; as discussed above, the boundary conditions of the simulations render them directly comparable to one growth cycle. There is, of course, nothing inherent in the continuous processes simulated by numerical models that can produce the required discontinuity of growth, and we must accept the hypothesis that growth stops altogether when ΔT_I becomes very small and resumes only after a significant ΔT_I is imposed. All simulated zoning profiles for one cycle of growth have the general shape shown in Fig. 3. It is easily conceived that a sharp drop of An content occurs in the crystal at the initiation of growth due to the high velocity. If a smooth oscillation profile is to be generated, it will occur by gradual rise of crystal An content back toward the equilibrium value as velocity decreases (A.T. Anderson, personal communication, has also noted this conclusion). In fact, only a limited indication of this rise is found in simulations, and the crystal composition may never reach the equilibrium value while growth continues. Thus, repeated growth cycles should produce asymmetrical, An-rich spikes probably similar in shape to those shown in Fig. 13. Oscillatory zoning profiles created by this growth process of diffusion and re-nucleation match neither the profiles predicted by Bottinga et al. (1966) and Sibley et al. (1976), nor observed profiles. The natural, oscillatory profile shown in Fig. 16, and those shown by Sibley et al. (1976) and Loomis and Welber (1982), lack the regular periodicity or consistent morphology expected to be produced by the periodic growth mechanism.

As Vance (1962) emphasizes, other mechanisms capable of producing oscillatory undercooling, such as periodic oscillation of P_{H_2O}, temperature, or perhaps P_{total}, require repeated rapid mass movement that renders them unlikely candidates for such a common process. In particular, the effect of periodic fracturing of the magma chamber and loss of water from the magma could affect water content very near the crystallization wall, but the slow diffusion rate of water would delay and attenuate variations of water content in the interior. Rapid convection within the magma chamber would be expected to change ΔT_B by only a few degrees in view of the small effect of P on the liquidus and the small adiabatic gradient of melts (Loomis and Welber 1982).

Another explanation for oscillatory zoning is the perturbation by local convection (on the scale of mm) of diffusion gradients developed adjacent to growing crystals. The water gradients generated adjacent to a growing crystal are a possible source of density gradient that could induce local convection. Shaw (1974, p. 165) gives an approximate method of calculating the maximum velocity of vertical boundary layer flow of melt along a surface in response to a gradient of water mass fraction normal to the surface. The maximum vertical velocity that would result adjacent to a 0.5 cm high crystal face was calculated for several simulations using the transport coefficient, average viscosity, and water gradient at 0.1 mm growth from the simulations, and approximate values for α_c of 1 and densities of 2.5 for granodiorite and 2.9 for basalt. At 30° C ΔT_B, the calculated vertical velocity is about 2.4 orders of magnitude greater than the simulated growth velocity for a granodiorite melt with 5 wt.% water, and 1.7 orders of magnitude greater for a melt with one wt.% water. For a basalt at a ΔT_B of 30° C and one wt.% water, the maximum vertical velocity is 1.8 orders of magnitude greater than growth. While there are numerous uncertainties in the analysis, it is difficult to avoid the conclusion that the density gradients generated adjacent to growing phenocrysts in hydrous melts at geologically-reasonable undercoolings can induce local convection. The gradient of the residual component in basic, low viscosity melts may also be capable of inducing convection in dry melts, but the data do not exist to evaluate this proposition quantitatively.

Figure 2 illustrates how local convection could cause oscillatory zoning. The conditions at the surface of a growing crystal might be represented by Loop 2, and the crystal forming has composition C. Convective motions would remove the excess concentrations of the residual component and water at the interface caused by growth and would allow the crystal composition to migrate back toward A. Because heat flow is so rapid, the process could be essentially isothermal at T_1. Thus, the crystal composition would migrate between A and C as the rate of convection varied.

I conclude that periodic convection over distances of a few mm is probably reponsible for most of the oscillatory zoning in igneous crystals. Periodic convective overturn would depend on a host of geochemical and geometric factors, but is expected to be most pronounced on the fastest growing crystal faces where diffusion gradients would be best developed, and can explain the irregular oscillatory zoning characteristic of these growth directions. Oscillatory zoning in volcanic pyroxenes has been reported by Smith and Carmichael (1969) and Downes (1974). It is significant that the elements showing the greatest variation in minerals are Al and Ti, expected to have low diffusivities in the melt, and that zoning is prominent only in pyroxenes that could have had high growth rates. Oscillatory zoning in minerals other than plagioclase and pyroxene may be rare because elements are partitioned more equally between melt and crystal, the minerals are less common in rapidly-cooled, low viscosity melts, and crystals may be homogenized after growth by intracrystalline diffusion.

Effect of Growth Rate on Partitioning of Trace Elements

The estimated diffusivities of Sr, Ba, Rb, K, and Cs, compiled by Magaritz and Hofmann (1978), and the growth velocities determined here can be used to estimate the maximum enrichment of these elements at a crystal face if they were entirely excluded from the crystal. Because the diffusivities of these elements are several orders of magnitude greater than that assumed for water in these simulations, the rather small accumulations of water predicted indicates that there will be negligible concentration of these elements at the crystal face; trace elements such as Ti or possibly Ni, with very low diffusivity, could show significant enrichment. Thus, it is unlikely that plagioclase grown under plutonic conditions will show the disequilibrium partitioning of trace elements discussed by Albarede and Bottinga (1972). Lindstrom et al. (1979) have produced trace element enrichment adjacent to much faster growing olivine.

Major Zoning

It is apparent from Fig. 11 that discontinuities in zoning or plateau or reverse zoning in plagioclase cannot be explained by an equilibrium fractionation model. The common occurence of irregular and reverse zoning in plagioclase in plutonic rocks indicates that plagioclase commonly grows under disequilibrium conditions. The simulations of disequilibrium growth combined with fractionation (for example, Fig. 14) suggest that undercooling has the following effects on fractionation profiles: (1) a rapid increase of undercooling causes a sharp drop in An content; (2) normal zoning is produced if undercooling is maintained during growth; and (3) reverse zoning is produced if undercooling decreases during growth.

The initial development of undercooling probably occurs at the inception of plagioclase growth because substantial undercooling may be required for nucleation, as indicated by the work of Swanson (1977). After growth begins, the change of undercooling will depend on the relative rate of change of temperature and the change of liquidus temperature of plagioclase caused by fractionation of the melt. It is reasonable to expect that the temperature of a magma will decrease during crystallization, although it is possible that some warming could occur due to released heat of crystallization if significant undercooling is necessary to nucleate crystals. The depression of the liquidus temperature of plagioclase in response to plagioclase crystallization will be enhanced if water is present in the melt and will be reduced if other phases crystallize and remove the residual component. Another consideration is illustrated by the thermal curves of Fig. 12. A small undercooling will produce the widest zoning band if it occurs early in the crystallization history because a large amount of pla-

gioclase must crystallize before the melt is fractionated enough to significantly decrease the liquidus temperature. Conversely, it will be difficult to detect the effects of undercooling on zoning during late stages of crystallization, especially considering the added complications of groundmass nucleation.

Overall, the simulations of plagioclase crystallization in granodiorite (Figs. 14 and 15) support the following conclusions. Phenocrysts of plagioclase growing with few other crystals should be normally zoned if they develop in rapidly-cooled environments, but they should show increasing reverse zoning in environments with slower cooling rates or more hydrous (but undersaturated) magmas. After plagioclase is joined by other crystallizing phases or saturation of water is reached, more normal zoning should be produced.

The presence of discontinuities in zoning or reverse zoning indicates that the composition of plagioclase may deviate significantly from equilibrium with the melt. Indeed, the model of phenocryst growth proposed here requires that the crystals be out of equilibrium with the bulk melt throughout much of their growth history. Consequently, geothermometers based on plagioclase composition must be applied with great reservation.

Acknowledgments. The author is indebted to R.J. Kirkpatrick. M.J. Drake, C.W. Burnham, and A. Navrotsky who aided in the development of earlier work on which these models are based. R.J. Kirkpatrick suggested to me long ago that oscillatory zoning was caused by local convection around crystals. D. O'Donnell and R. Strauss contributed through discussion and valuable assistance in programming. Research was supported by the Earth Sciences Section, National Science Foundation, NSF Grant EAR 7904108 and the University of Arizona. Computer facilities were provided by the University Computer Center.

References

Albarede F, Bottinga, Y (1972) Kinetic disequilibrium in trace element partitioning between phenocrysts and host lava. Geochim Cosmochim Acta 35:141–256

Bottinga Y, Kudo A, Weill D (1966) Some observations on oscillatory zoning and crystallization of magmatic plagioclase. Am Mineral 51:792–806

Burnham, CW (1975) Thermodynamics of melting in experimental silicate-volatile systems. Fortschr Mineral 52:101–118

Burnham CW (1979) The importance of volatile constituents. In: Yoder HS (ed) A Fiftieth Anniversary appraisal of Bowen's evolution of the igneous rocks. Princeton University, Princeton, NJ, pp 439–482

Downes MJ (1974) Sector and oscillatory zoning in calcic augites from Mt. Etna, Sicily. Contrib Mineral Petrol 47:187–196

Fenn PM (1977) Nucleation and growth of alkali feldspar from hydrous melts. Can Mineral 15:135–161

Flood H, Knapp WJ (1968) Structural characteristics of liquid mixtures of feldspar and silica. J Amer Ceram Soc 51:259–263

Greenwood HJ, McTaggart KC (1957) Correlation of zones in plagioclase. Amer J Sci 255:656–666

Harloff C (1927) Zonal structure in plagioclase. Leidse Geol Meded 2:99–114

Hess PC (1970) Polymer model of silicate melts. Geochim Cosmochim Acta 35:289–306

Hills ES (1936) Reverse and oscillatory zoning in plagioclase feldspars. Geol Mag 73:49–56

Hopper RW, Uhlmann DR (1974) Solute redistribution during crystallization at constant velocity and constant temperature. J Crystal Growth 21:203–213

Jambon A (1979) Diffusion of water in obsidian. Eos 60:409 (abs)

Kirkpatrick RJ, Robinson GR, Hays JF (1976) Kinetics of crystal growth from silicate melts: Anorthite and diopside. J Geophys Res 81:5715–5720

Kirkpatrick RJ, Klein L, Uhlmann DR, Hays JF (1979) Rates and processes of crystal growth in the system anorthite-albite. J Geophys Res 84:3671–3676

Lindstrom DJ, Lofgren GE, Haskin LA (1979) Experimental studies of kinetic effects on trace element partitioning. Eos 60:402 (abs)

Lofgren, G (1972) Temperature induced zoning in synthetic plagioclase feldspar. In: MacKenzie WS (ed) The feldspars. Univ of Manchester Press, Manchester, pp 362–377

Loomis TP (1979) An empirical model for plagioclase equilibrium in hydrous melts. Geochim Cosmochim Acta 43:1753–1759

Loomis TP (1981) An investigation of disequilibrium growth processes of plagioclase in the system anorthite-albite-water by methods of numerical simulation. Contrib Mineral Petrol 76:196–205

Loomis TP, Welber PW (1982) Crystallization processes in the Rocky Hill Granodiorite Pluton, California: An interpretation based on compositional zoning of plagioclase. Contrib Mineral Petrol 81:230–239

Maaloe S (1976) The zoned plagioclase of the Skaergaard intrusion, east Greenland. J Petrol 17:398–419

Margaritz M, Hofmann AW (1978) Diffusion of Sr, Ba and Na in hydrous melts. Geochim Cosmochim Acta 42:595–606

Rutter JW, Chalmers B (1953) A prismatic substructure formed during the solidification of metals. Can J Phys 31:15–39

Shaw HR (1974) Diffusion of H_2O in granitic liquids. In: Hofmann AW, Giletti BJ, Yoder HS Jr, Yund RA (ed) Geochemical Transport and Kinetics. Carnegie Inst Washington Publ 634:139–170

Sibley DF, Vogel TA, Walker BW, Byerly G (1976) The origin of oscillatory zoning in plagioclase: A diffusion and growth controlled model. Am J Sci 276:275–284

Swanson SE (1977) Relation of nucleation and crystal-growth rate to the development of granitic textures. Am Mineral 62:966–978

Smith AL, Carmichael ISE (1969) Quaternary trachybasalts from S.E. California. Am Mineral 54:909–923

Taylor M, Brown GE Jr (1979) Structure of mineral glasses – I. The feldspar glasses $NaAlSi_3O_8$, $KAlSi_3O_8$, $CaAl_2Si_2O_8$. Geochim Cosmochim Acta 43:61–76

Vance JA (1962) Zoning in igneous plagioclase: Normal and oscillatory zoning. Am J Sci 260:746–760

Watson EB (1979) The effect of dissolved water on cesium diffusion in molten granite. Eos 60:402 (abs)

Wiebe RA (1968) Plagioclase stratigraphy: a record of magmatic conditions and events in a granite stock. Am J Sci 266:670–703

Received May 11, 1982; Accepted October 10, 1982